Research Square

Preprints are preliminary reports that have not undergone peer review.
They should not be considered conclusive, used to inform clinical practice,
or referenced by the media as validated information.

PlasticFADE: A predictive model for plastic fragmentation and degradation in the environment

Yibo Tang
CIRAIG, Polytechnique Montreal
Nadim Saadi
CIRAIG, Polytechnique Montreal
Jérôme Lavoie
CIRAIG, ESG UQAM
Anne-Marie Boulay
anne-marie.boulay@polymtl.ca

CIRAIG, Polytechnique Montreal

Research Article

Keywords: Environmental fate modeling, Life cycle impact assessment, Plastic lifespan, Plastic pollution, Plastic weathering, Secondary microplastics, Persistence

Posted Date: April 24th, 2026

DOI: https://doi.org/10.21203/rs.3.rs-9347297/v1

License: This work is licensed under a Creative Commons Attribution 4.0 International License.
Read Full License

Additional Declarations: No competing interests reported.

PlasticFADE: A predictive model for plastic fragmentation and degradation in the environment

Yibo Tang [a], Nadim Saadi [a], Jérôme Lavoie [b], Anne-Marie Boulay *[a]

Authors affiliations:

[a] CIRAIG, Department of Chemical Engineering, Polytechnique Montréal, 3333 Queen Mary Road, suite 310, Montréal, Québec, H3V 1A2, Canada

[b] CIRAIG, Department of Strategy and Corporate Social Responsibility, ESG UQAM, 3333 Queen Mary Road suite, 310, Montréal, Québec, H3V 1A2, Canada

Corresponding author: Anne-Marie Boulay (anne-marie.boulay@polymtl.ca)

Abstract

Plastics are widespread across the globe, posing risks to environmental and human health. Fragmentation and degradation are key processes that govern the environmental fate and impacts of plastics, yet their rates remain poorly quantified. Life cycle assessment (LCA) is widely recognized as the standard framework for comprehensively evaluating the environmental performance of products and services. Accurately capturing the fate of plastics in natural environments therefore represents a critical priority for impact assessment modeling. However, the degradation and fragmentation mechanisms governing plastic polymer behavior remain poorly quantified in current life cycle impact assessment (LCIA) models, limiting their capacity to characterize the potential biodiversity impacts arising from plastic emissions to natural environments. In this study, experimental data on plastic fragmentation and degradation were systematically compiled from the literature. Using these data, PlasticFADE was developed as the first iteration of an empirical model to predict polymer-specific rate constants in various environmental compartments. The model predictions reveal that the rate constants vary considerably across polymers and compartments. Estimated lifespans of plastics range from several decades to over a millennium. Beaches are identified as hotspots for both fragmentation and degradation, whereas plastics are most likely to remain intact in the water column. Criteria are proposed for evaluating the reliability of the model outputs, which should be interpreted with due caution. Despite its limitations, the model offers valuable insights into plastic fate processes and offers significant potential for improving current LCIA methods for plastic emissions assessment.

Keywords

Environmental fate modeling, Life cycle impact assessment, Plastic lifespan, Plastic pollution, Plastic weathering, Secondary microplastics, Persistence

1. Introduction

Plastic pollution is ubiquitous, reaching even the most remote areas of the planet, and has raised increasing concerns regarding its potential impacts on environmental and human health (Bergmann et al., 2019). It is estimated that over 200 million metric tons of plastic waste are generated globally each year (Law et al., 2020). Plastics are commonly categorized by size into macroplastics (> 5 mm), microplastics (1 μm–5 mm), and nanoplastics (< 1 μm) (Merga et al., 2020). They undergo slow transformation processes under natural conditions: *fragmentation* refers to the physical breakdown of larger plastic items into smaller pieces, while *degradation* typically involves chemical or biological conversion into non-plastic substances (e.g., carbon dioxide, oligomers), resulting in a net loss of plastic mass over decades to centuries (Woods et al., 2021; Pfohl et al., 2022). These processes are primarily driven by individual or combined environmental stressors—such as ultraviolet (UV) radiation, mechanical abrasion, and microbial activity—depending on the environmental compartment in which the plastics reside (Zhang et al., 2021).

Fragmentation and degradation are key processes governing the environmental fate and impacts of plastics. With the aim of fully capturing the detrimental effects of plastics in the environment, and comparing the environmental performance of plastic materials with alternatives, accurately quantifying fragmentation and degradation processes is crucial. Life cycle assessment (LCA) is a methodology for quantifying the potential impacts of a product or service on ecosystem quality and human health across its entire life cycle. Within the LCA context, characterization factors (CFs) have been developed for marine microplastics (Corella-Puertas et al., 2023; Saadi et al., 2025), approximately 70% of which are estimated to arise from the fragmentation of macroplastic debris, i.e., secondary microplastics (Boucher & Friot, 2017). Quantifying plastic fragmentation and degradation rates is critical for linking emission data to the impact assessment of microplastics, especially considering that the fate of plastic pieces in the environment is what drives the overall impact of plastic emissions (Corella-Puertas et al., 2023; Saadi et al., 2025; Louvet et al., 2026). Fragmentation and degradation processes have also been shown to significantly influence the results of LCAs involving plastic materials (UNEP, 2022; Corella-Puertas et al., 2023). Fragmentation governs the generation of microplastics following leakage of macroplastics into the environment (i.e., the source term), while degradation dictates their environmental fate and removal (i.e., the loss term) (Hajjar et al., 2024).

In recent years, an increasing number of experimental studies have investigated plastic fragmentation and degradation, the majority of which have been conducted under controlled laboratory conditions. However, the data are reported in various formats. In addition to mass loss percentages, fragmentation is described in some studies by the mass (or number and size) of the resulting particles (Reineccius et al., 2023; Song et al., 2022), whereas degradation is sometimes quantified using specific surface degradation rates (SSDRs) expressed in μm/year (Chamas et al., 2020; Maga et al., 2022). Fragmentation and degradation have been incorporated into models such as The Full Multi, FRAGMENT-MNP, and SimpleBox4Plastic (Domercq et al., 2022; Harrison et al., 2025; Quik et al., 2023). However, these models do not account for variations in fragmentation and degradation rates across different emission scenarios (i.e., polymer and environmental compartment) and are not applicable to macroplastic emissions. The SSDR approach can derive compartment specific degradation rates, but the results cannot be extrapolated to other environmental compartments, as the results reflect specific experimental conditions. Also, specific models have been developed to simulate fragmentation and degradation under a single environmental stressor (An et al., 2021; Sipe et al., 2022). However, in certain environments (e.g., beaches), multiple stressors act concurrently to promote plastic breakdown. To address these gaps, this study develops an empirical, polymer-specific model that quantifies fragmentation and degradation rates across all major environmental compartments as a

74 function of compartment-specific stressors, providing globally applicable parameters for integration into
75 LCIA frameworks.

2. Materials and Methods

2.1. Model definition

Although terms such as *dissolution* and *dissociation* are also commonly used in the literature, we adopt the terms *fragmentation* and *degradation* to ensure consistency with the terminology used in the framework for assessing marine litter impacts developed by the MarILCA working group (Woods et al., 2021). This work begins with selecting the fragmentation and degradation processes to be included (Table 1). Biodegradation refers to the conversion of plastics by microbes into simpler compounds, while trophic breakdown denotes the transformation of plastics within the digestive systems of living organisms. Hydrolysis (degradation via the cleavage of chemical bonds through reaction with water molecules) is not included in the model for two main reasons. First, it is limited to polymers containing hydrolyzable linkages such as ester or amide bonds. Second, it contributes negligibly to the overall mass loss. For PLA, Meng et al. (2025) reported a mass loss of 0.13% after 30 days of hydrolysis, whereas substantially greater losses were observed in biodegradation studies: 3.37% in 35 days at 30°C (Mistry et al., 2022) and 2.65% in 28 days, at 37°C (Yottakot & Leelavatcharamas, 2019). For PET, hydrolysis is negligible under normal conditions and occurs primarily in strongly acidic or alkaline environments, or at elevated temperatures above 200 °C (Yang et al., 2021). This is in line with previous work showing that hydrolysis, while always present, remains slow relative to other degradation pathways under most environmental conditions (Colwell et al., 2023).

Table 1. Inclusion status of common fragmentation and degradation processes in the model

Process	**Contribution**	**Modeled?**	**Environmental stressor & quantified stress / Justification for exclusion**
Photooxidation	Fragmentation & Degradation	Yes	UV radiation, UV intensity [W/m^2]
Mechanical fragmentation	Fragmentation	Yes	Mechanical abrasion, Mechanical power [mW]
Biodegradation	Degradation	Yes	Microbial activity, Microbial concentration [CFU/mL]
Thermal oxidation	Degradation	No	Requires temperatures well beyond environmentally relevant ranges
Hydrolysis	Degradation	No	Applies only to specific polymer types; Contributes negligibly to mass loss
Trophic breakdown	Fragmentation & Degradation	No	Quantification limited by interspecies variation and physiological complexity
Photocatalytic oxidation	Fragmentation & Degradation	No	Relies on added photocatalysts that are not present in natural environments

The primary factors influencing plastic fragmentation and degradation rates include polymer type, size and shape of the plastic object (more specifically, its surface area to volume ratio–SA:V), and the environmental compartment in which it resides. A high SA:V means that a large surface is available for surface degradation (compared to the volume), potentially increasing degradation rates (Maga et al., 2022). Accordingly, the

model addresses a range of commodity polymers (HDPE, LDPE, PE, PP, PS, PET, and EPS), sizes (macro-, micro-, and nanoplastics), shapes (spheres, cubes, films, fibers, and non-uniform shapes), and environmental compartments (air, topsoil, subsoil, beach, water surface, water column, and sediment). Polyethylene is categorized as HDPE (> 0.94 g/cm^3), LDPE (< 0.94 g/cm^3), and PE (~ 0.94 g/cm^3). While HDPE and LDPE samples were typically prepared by cutting postconsumer products, PE samples were more often obtained directly from manufacturers. Subsoil is distinguished from topsoil by the absence of UV exposure, negligible mechanical stress, and reduced biological activity (Table S3, Supporting Information 1). The water surface compartment denotes the upper layer of rivers, lakes, and oceans where photochemical oxidation can take place, while UV-shielded deeper zones are classified as the water column compartment. In this study, no distinction is made between freshwater and seawater regarding their effects on fragmentation and degradation, nor between freshwater and marine sediments. The next step is to parameterize fragmentation and degradation rates as functions of the influencing factors. An empirical rather than mechanistic modeling approach is adopted for two main reasons: (1) the inherent complexity of the system, arising from multiple environmental stressors (Table 1); and (2) the focus on predicting plastic fragmentation and degradation rates rather than elucidating molecular-level mechanisms.

The proposed model, PlasticFADE (Plastic Fragmentation And Degradation in the Environment), introduces a novel approach that differentiates plastic fragmentation and degradation rates according to polymer type and environmental compartment. The model is calibrated separately for each polymer, with environmental variability captured through three parameters denoting distinct environmental stresses. Recent studies have modeled fragmentation and degradation dynamics using first-order kinetics (Auta et al., 2022; Pfohl et al., 2022), and demonstrated that a general power law relationship ($y = ax^k$) effectively captures the linear and non-linear influence of environmental factors on rate constants (An et al., 2021). Building on these approaches, we developed two sets of empirical model equations, calibrated through curve fitting of experimental data compiled from the literature. The set identified as more suitable based on comparative analysis is presented in Eqs. 1 and 2, while the alternative set and the rationale for the final decision are provided in Section S4 of Supporting Information 1.

$$k_{frag,i,j} = a_i \cdot s^{\delta_i} \cdot \left(b_i \cdot {I_j}^{\alpha_i} + c_i \cdot {P_j}^{\beta_i}\right) \#(1)$$

$$k_{degr,i,j} = x_i \cdot s^{\tau_i} \cdot \left(y_i \cdot {I_j}^{\theta_i} + z_i \cdot {C_j}^{\eta_i}\right) \#(2)$$

$k_{frag,i,j}$ and $k_{degr,i,j}$ (d^{-1}) denote fragmentation and degradation rate constants, respectively, for polymer i in compartment j. These rate constants are expressed in $kg_{mass\ loss} . {kg_{in\ compartment}}^{-1} . d$, representing the relative mass loss per day due to fragmentation or degradation. Among the input variables, s (cm^{-1}) refers to the SA:V of a plastic item, while I_j (W/m^2), P_j (mW), and C_j (CFU/mL) denote the UV intensity, mechanical power, and microbial concentration, respectively, to which the plastic item is exposed in compartment j. Parameters with subscript i are empirical constants specific to polymer i, where the coefficients capture the linearity and the exponents the non-linearity between the input variables and the rates. The coefficients a_i and x_i scale the overall magnitude of fragmentation and degradation, respectively, with larger values reflecting a polymer more susceptible to degradation or fragmentation. The SA:V exponents (δ_i and τ_i) determine how strongly the SA:V ratio influences the rates; a larger exponent indicates that fragmentation or degradation is more pronounced in items with high SA:V (e.g., thin films). The photo-fragmentation and photo-degradation coefficients (b_i and y_i) and their respective exponents (α_i and θ_i) govern the UV response, where a larger coefficient and exponent reflect greater photosensitivity. Similarly,

c_i and β_i describe the sensitivity of fragmentation to mechanical stress, while z_i and η_i describe the sensitivity of degradation to microbial concentration.

2.2. Data collection and processing

To obtain data for estimating polymer-specific empirical constants, we first identified relevant articles in the Web of Science database using a combination of keywords related to polymer type, mass loss, and process (i.e., fragmentation, degradation, and alternative terms such as breakdown, decomposition, and aging). Data were extracted from the identified articles, stored in a database, and classified based on their relevance to fragmentation or degradation. Details on the data collection procedure are given in Section S1 of Supporting Information 1.

In the data processing stage, the collected information was converted into individual data points for model calibration. Data explicitly attributable to either fragmentation or degradation were processed, whereas data reported solely as inseparable mass loss were excluded from model development. In addition, data from control groups were reviewed and documented, and, where appropriate, subtracted from test group results to correct for mass loss due to the leaching of chemicals and other impurities. As shown in Eqs. 1 and 2, each model equation has four quantifiable variables: $k_{frag,i,j}$, s, I_j, P_j for fragmentation, and $k_{degr,i,j}$, s, I_j, C_j for degradation. The rate constants, $k_{frag,i,j}$ and $k_{degr,i,j}$, were calculated from reported mass loss and exposure duration. When data on the generated fragments were provided, mass loss was estimated as the ratio of the cumulative volume or mass of the fragments to the initial volume or mass of the plastic item. The first-order reaction rate equation (Eq. 3) serves as the basis for calculating the rate constants (Eqs. 4–6). Here, $r_{m,f}$ is the fragmentation rate (kg/d), m is the remaining plastic mass (kg), m_t is the plastic mass at time t (kg), W is the mass loss relative to the original plastic item due to fragmentation (-), and t is the exposure duration (d). The same procedure was applied to the collected degradation data.

$$r_{m,f} = \frac{dm}{dt} = -k_{frag} m \quad \#(3)$$

$$m_t = m_0 e^{-k_{frag} t} \quad \#(4)$$

$$W = \frac{m_0 - m_t}{m_0} = 1 - e^{-k_{frag} t} \quad \#(5)$$

$$k_{frag} = -\frac{ln\ ln\ (1 - W)}{t} \quad \#(6)$$

For the remaining variables in Eqs. 1 and 2, s (cm^{-1}) can be derived directly from the physical dimensions of the plastic item. In contrast, quantifying the environmental stresses (i.e., I_j, P_j, C_j) to which plastic was exposed necessitates additional modeling. To ensure comparability across diverse experimental conditions, environmental stresses are expressed in consistent units: UV intensity in watts per square meter (W/m^2), mechanical power in milliwatts (mW), and microbial concentration in colony-forming units per milliliter (CFU/mL). Details on the quantification of environmental stresses are provided in Section S2 of Supporting Information 1.

2.3. Model calibration

Model equations were calibrated against data points from the preceding step using the curve_fit() function within Python's SciPy library, which employs the nonlinear least squares minimization algorithm. A general

guideline for robust parameter estimation in nonlinear curve fitting suggests a minimum of 10 data points per parameter. As each model equation contains six empirical constants, this would necessitate at least 60 data points. However, due to pronounced data scarcity, an absolute minimum threshold was applied: curve fitting was conducted for polymers with at least six available data points. Given that the rate constants span several orders of magnitude, curve fitting was performed in logarithmic space, i.e., the model equations and the data points were log-transformed prior to fitting. In addition, an iterative fitting process was employed, which terminated when the relative difference between successive parameter estimates fell below 0.1% for all empirical constants. The quality of fit was evaluated both visually, by comparing model predictions with reported values in plotted figures, and numerically, via computing coefficients of determination (see Section S4.2 of Supporting Information 1). A key assumption in this step was that the input variables—SA:V and environmental stresses—remained constant, given the relatively short duration of the experimental studies compiled in the database (≤ 18 months).Once fragmentation or degradation parameters have been calibrated for a given polymer, the model can be applied to predict the corresponding rate constants of that polymer in compartments characterized by different environmental stressors (different microbial concentration, UV and mechanical stress). Further, users of the model could introduce additional equations to quantify the change of SA:V over time (and therefore changing k_{frag} and k_{deg} over time). This was not done in this work, as it is difficult to estimate SA:V changes, as models predicting the size and shape of the fragmenting and degrading particles do not yet exist.

2.4. Model application

The rate constants computed by PlasticFADE can be further used to estimate the residence time of a plastic object within a specific environmental compartment and to simulate its mass transformation pathways. For this application, the system was modeled using first-order kinetics, assuming no additional input for t > 0 and no transfer between compartments. In addition, it was assumed that all particles originating from the fragmentation of macroplastics are classified as micro- or nanoplastics, thereby excluding the formation of macro-sized fragments. This assumption is consistent with common experimental practice, which typically reports only the mass of the generated micro- and nanoplastics. Eqs. 7 and 8 describe the processes modeled within the system. Both processes are applicable to macroplastic emissions, while only the latter is relevant for direct emissions of micro- and nanoplastics (hereafter collectively referred to as "microplastics" within this section for simplicity). Residence time was characterized using two measures: t_{macro}, the time required for the mass of macroplastics to decline to 0.1% of its initial value (the rest having fragmented or degraded); and t_{total}, the time at which only 0.1% of the initial mass remains in plastic form (the rest having degraded). Table 2 presents the mass balance equations and their analytical solutions for estimating the residence time and the masses of macroplastics (A), microplastics (B), and degradation products (C) after a given exposure duration (m_0: initial mass of the emitted plastics; t: time spent in the compartment). m_θ denotes the mass threshold used to represent complete removal under first-order kinetics. In this study, it is defined as 0.1% of the m_0, as specified above.

$$\text{Macroplastics} \xrightarrow{\text{fragmentation \& degradation}} \text{Microplastics} + \text{Degradation products} \quad (7)$$

$$\text{Microplastics} \xrightarrow{\text{fragmentation \& degradation}} \text{Smaller microplastics} + \text{Degradation products} \quad (8)$$

Table 2. Mathematical representation of mass balance, mass distribution, and residence time

Model components	Macroplastic emission	Microplastic emission
Mass balance (Differential)	$\frac{dm_A}{dt} = -(k_{frag} + k_{degr})m_A$ $\frac{dm_B}{dt} = k_{frag}m_A - k_{degr}m_B$ $\frac{dm_C}{dt} = k_{degr}m_A + k_{degr}m_B$	$\frac{dm_B}{dt} = -k_{degr}m_B$ $\frac{dm_C}{dt} = k_{degr}m_B$
m_A	$m_0 e^{-(k_{frag}+k_{degr})t}$	–
m_B	$m_0\left(e^{-k_{degr}t} - e^{-(k_{frag}+k_{degr})t}\right)$	$m_0 e^{-k_{degr}t}$
m_C	$m_0\left(1 - e^{-k_{degr}t}\right)$	$m_0\left(1 - e^{-k_{degr}t}\right)$
t_{macro}	$-\frac{ln\ (m_\theta/m_0)}{k_{frag} + k_{degr}}$	–
t_{total}	$-\frac{ln\ (m_\theta/m_0)}{k_{degr}}$	$-\frac{ln\ (m_\theta/m_0)}{k_{degr}}$

2.5. Model evaluation

The model evaluation stage involves uncertainty analysis, reliability assessment, and validation of the model results. To characterize the uncertainty in the model results, we first quantified parameter uncertainty during curve fitting by computing the Fisher Information Matrix (FIM), derived from the Jacobian of the residuals (Sharp et al., 2022). In this study, computation of FIM was conducted by assuming log-normally distributed errors. Next, we derived the standard deviations (SDs) of the fitted parameters from the inverse of the FIM, assuming local linearity of the model near the optimal solution (Ly et al., 2017). We then sampled the fitted parameters from their distributions (i.e., point estimate ± one SD) and propagated these samples through the model via Monte Carlo simulations (N = 10 000). Finally, we derived 95% confidence intervals (CIs) from the resulting distributions of the modeled rate constants, providing a quantitative measure of uncertainty in the model estimates.

Because this study employs an empirical modeling approach, it is essential to assess the level of confidence associated with each model output. To this end, two assessment criteria were established: (1) the 95% CI of the modeled rate constant spans less than two orders of magnitude; and (2) all fitted parameters meaningfully contribute to the predicted rate constant—parameters whose estimated values are effectively zero (≤ 1E-10) are considered to have negligible influence and thus indicate low confidence. A color-coding scheme was applied to indicate compliance with these criteria—green when both are satisfied, orange when only one is satisfied, and red when neither is satisfied—corresponding to high, moderate, and low levels of confidence, respectively. This scheme provides an initial indication of the reliability of the model outputs. To further validate the model results, the predicted rate constants and residence times were compared with values reported in the literature and with datasets not used during model calibration.

3. Results and Discussion

3.1. Data sources and plastic material descriptions

The references used to collect data are reported in Supporting Information 2 under Env. stresses, Calibration and References tabs. Plastic materials used in the experiments serving as data sources originate from diverse sources. They consist predominantly of pre-production pellets, shaped materials, and pre-consumer packaging available on the market, with post-consumer waste more rarely represented. A total of 34 experiments were identified as respecting the criteria described in Section 2.2 of this manuscript and Section S1 of Supporting Information 1.

3.2. Fragmentation and degradation rate constants

Empirical constants for the fragmentation of PP, PS, and EPS, as well as for the degradation of PP, PS, PET, HDPE, LDPE, and PE, were obtained through curve fitting. These fitted parameters enable PlasticFADE to compute polymer-specific rate constants for each environmental compartment, based on the UV intensity, mechanical power, and microbial concentration characteristic of that compartment. The derivation of the representative values for each compartment is detailed in Section S3 of Supporting Information 1. As an illustrative example, we assume an emission of plastic food containers (4 cm tall, 11 cm wide, and 0.8 mm thick) and present the modeled rate constants across different polymer-compartment combinations (Figs. 1 and 2). The rate constants are provided only for polymers for which at least six data points were available to proceed with the curve fitting, as stated in Section 2.3 (PP, PS and EPS for fragmentation and PP, PS, PET, HDPE, LDPE and PE for degradation). An Excel implementation of the PlasticFADE model is provided in Supporting Information 2, along with the compiled database of plastic fragmentation and degradation and the datasets underlying the figures presented in the main text.

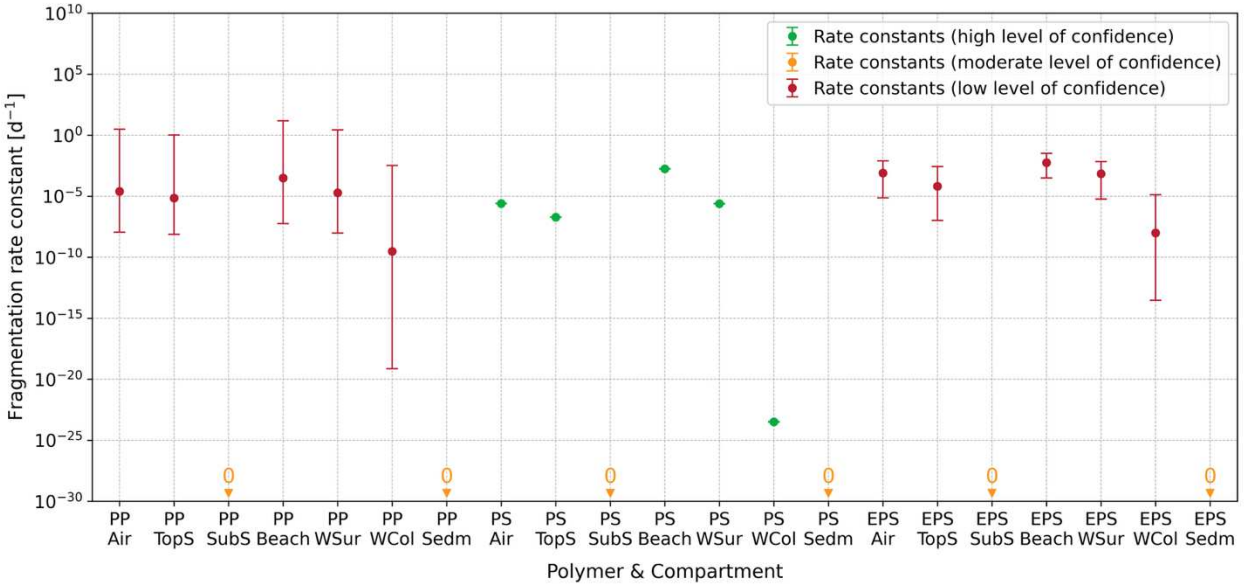


Figure 1. Fragmentation rate constants (± 95% CIs) estimated by PlasticFADE for a food container (height: 4 cm, diameter: 11 cm, thickness: 0.8 mm). Color-coding scheme integrated. TopS = topsoil, SubS = subsoil, WSur = water surface, WCol = water column, Sedm = sediment). Null fragmentation rates are obtained in compartments without UV or mechanical stress (subsoil and sediments).

In Figs. 1 and 2, the computed rate constants are shown on a logarithmic scale, spanning several orders of magnitude across different polymers and compartments. The error bars represent the 95% CIs for the rate constants, with narrower CIs reflecting lower uncertainty in the model outputs. For PS fragmentation and PE degradation, the CIs are not discernible at the plotted scale due to the very low standard deviations of the fitted parameters obtained during curve fitting. This likely results from the limited degrees of freedom (with the number of data points ≈ the number of unknown parameters) or the (often accidental) high internal consistency of the data. Except for these two unusual cases, fragmentation rate constants generally exhibit wider 95% CIs than degradation rate constants for two main reasons. First, fewer data points are available for fragmentation than for degradation, making the parameter estimates more sensitive to data variability and outliers and thus less statistically constrained. Second, whereas degradation was typically reported as mass loss, fragmentation was expressed in terms of the number and average size of generated fragments in some studies. Converting these metrics to equivalent mass loss introduces additional uncertainty into the parameter estimation.

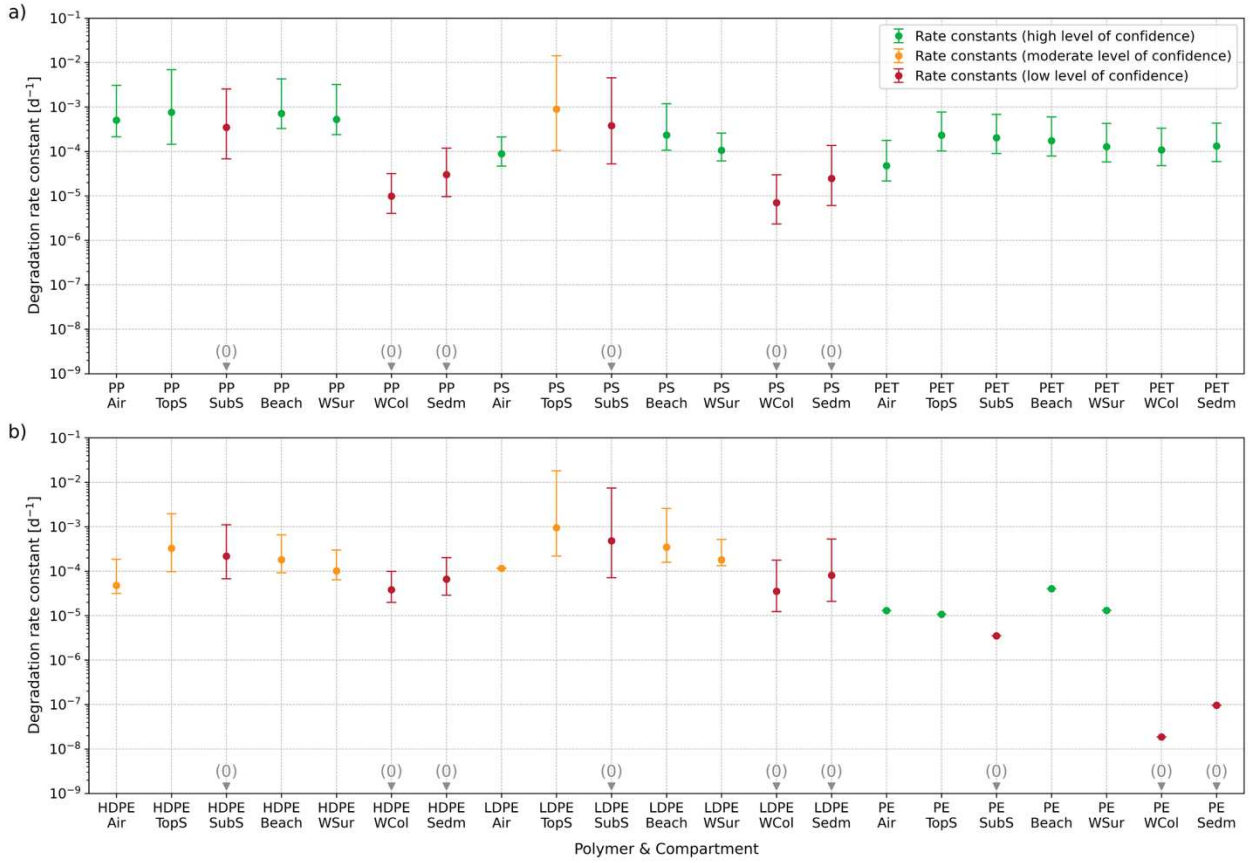


Figure 2. Degradation rate constants (± 95% CIs) estimated by PlasticFADE for a food container (height: 4 cm, diameter: 11 cm, thickness: 0.8 mm), for PP, PS, and PET (a) and HDPE, LDPE, and PE (b). Color-coding scheme integrated. TopS = topsoil, SubS = subsoil, WSur = water surface, WCol = water column, Sedm = sediment). For polymers without identified degrading enzymes, a value of (0) is assigned to represent degradation rates in UV-absent compartments, although the model still computes a degradation rate.

In addition to the uncertainty in the model outputs, Figs. 1 and 2 show that the rate constants depend on both

polymer and compartment. Fragmentation rate constants are zero in subsoil and sediment (with moderate level of confidence defined), since UV is absent and mechanical stress is negligible. EPS shows higher rate constants (i.e. faster fragmentation) than PP and PS across all compartments, except in subsoil and sediment. This outcome can be attributed to its highly porous structure, which makes it more prone to fragmentation than bulk plastics (Song et al., 2020). For degradation, the zero values shown in Fig. 2 are explained in the following section. LDPE consistently exhibits higher degradation rate constants than HDPE, likely due to its branched molecular structure, which reduces crystallinity and creates amorphous regions that are more susceptible to oxidative and enzymatic attack (Ghatge et al., 2020). As specified in Section 2.1, PE samples were primarily pristine materials obtained directly from manufacturers. This may explain their lower rate constants relative to HDPE and LDPE, as surface alterations occurring during the use phase likely reduce the material's resistance to degradation. At the compartment level, fragmentation and degradation hotspots do not necessarily coincide, because their rate constants are controlled by different environmental stressors. Topsoil—characterized by limited UV exposure and mechanical stress but high microbial activity— shows high degradation activity yet relatively low fragmentation activity. In contrast, the water column represents an environment where both processes will be significantly slower than in other compartments. Overall, the variability in the modeled rate constants highlights the strong influence of polymer and compartment on fragmentation and degradation.

3.3. Additional model results

Using the modeled rate constants and the equations in Table 2, residence times were estimated for the food containers described in the previous section. These estimates are not direct model outputs but are presented to illustrate the model results through more intuitive and interpretable metrics. Table 3 shows the estimated t_{macro} and t_{total} values for polymers with available fragmentation and degradation rate constants, namely PP and PS. t_{total} values for HDPE, LDPE, PE, and PET are given in Table S8 of Supporting Information 1. When the modeled fragmentation rate constant is considerably lower than the degradation rate constant (e.g., for PP and PS in topsoil), the food container undergoes degradation more rapidly than fragmentation. In such cases, most of the plastic mass is consumed via degradation before significant fragmentation occurs, resulting in the generation of very few fragments. This behavior is captured in the model predictions, where t_{macro} closely approximates t_{total}.

Table 3. Modeled rate constants and estimated lifespans of food containers (height: 4 cm; diameter: 11 cm; thickness: 0.8 mm) in different environmental compartments. Color coding denotes the level of confidence in the model outputs (green=high, orange=moderate, red=low; see Section 2.5 for details). The complete set of results is provided in Table S8 of Supporting Information 1.

Polymer	**Compartment**	k_{frag} **[d^{-1}]**	k_{degr} **[d^{-1}]**	t_{macro} **[yr]**	t_{total} **[yr]**	**95% CI_**t_{total} **[yr]**
PP	Air	2.48E-05	5.03E-04	36	38	6~89
PP	Topsoil	7.08E-06	7.61E-04	25	25	3~131
PP	Subsoil	0	3.48E-04	54 – ∞	54 – ∞	7~277 – ∞
PP	Beach	3.17E-04	7.16E-04	18	26	4~58
PP	Water surface	1.94E-05	5.26E-04	35	36	6~79
PP	Water column	2.98E-10	9.89E-06	1914 – ∞	1914 – ∞	595~4706 – ∞

PP	Sediment	0	3.02E-05	626 – ∞	626 – ∞	159~1969 – ∞
PS	Air	2.57E-06	8.82E-05	208	214	90~405
PS	Topsoil	1.91E-07	8.91E-04	21	21	1~180
PS	Subsoil	0	3.81E-04	50 – ∞	50 – ∞	4~362 – ∞
PS	Beach	1.79E-03	2.34E-04	9	81	16~177
PS	Water surface	2.46E-06	1.06E-04	175	179	73~310
PS	Water column	3.22E-24	7.01E-06	2698 – ∞	2698 – ∞	632~8081 – ∞
PS	Sediment	0	2.46E-05	770 – ∞	770 – ∞	139~3120 – ∞

To date, no plastic-degrading enzymes have been identified for PE (including HDPE and LDPE), PP, or PS (Chow et al., 2023; Tournier et al., 2023). Reported mass loss of these polymers in biodegradation studies thus mainly reflects the mineralization of short-chain fragments (e.g., monomers and oligomers) rather than the cleavage of polymer backbones. As a result, in compartments lacking UV radiation (i.e., subsoil, water column, and sediment), the degradation of PE, PP, and PS is expected to cease once the readily degradable compounds have been completely metabolized by microbes. This pattern is reflected by the zero values in parentheses in Fig. 2, indicating the affected polymers and compartments. Accordingly, the associated rate constants are assigned a low level of confidence, and the corresponding lifespans may theoretically extend to infinity (Table 3). Moreover, given that the rate constants for PS fragmentation and degradation are both considered robust (i.e., high level of confidence) in beach and water surface compartments (Table 3), Sankey diagrams were created to illustrate the estimated mass transformation pathways for PS food containers (Fig. 3). Comparison between Fig. 3a and Fig. 3b reveals that the formation of secondary microplastics strongly depends on the relative magnitudes of k_{frag} and k_{degr}. On the beach, where k_{frag} is greater than k_{degr}, secondary microplastics constitute a major fraction of the mass loss from the PS containers. In contrast, the accumulation of secondary microplastics is minimal at the water surface (with $k_{frag} << k_{degr}$), as the PS containers are much more prone to degradation than fragmentation.

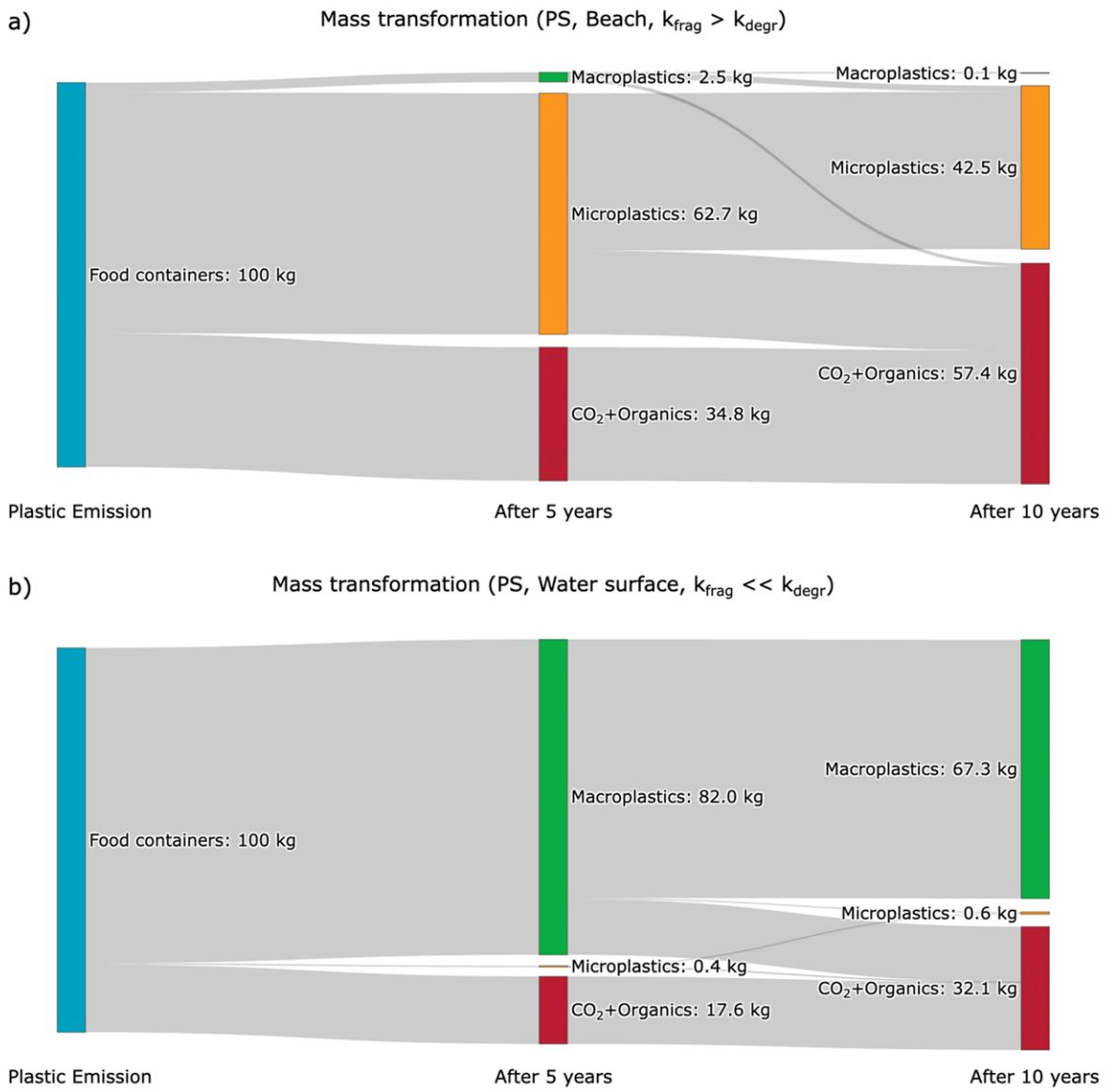


Figure 3. Predicted mass transformation of PS food containers a) on the beach and b) at the water surface

3.4. Validation of model results

In best practice modeling studies, the dataset is divided into one test and one validation subset to perform the cross-validation (Hastie et al., 2009). Considering the limited dataset in this study, this was not possible. Hence, model results, including the rate constants and the predicted lifespans, were validated against four types of reference data: (1) estimates reported in the literature; (2) measured total mass loss due to fragmentation and degradation combined; (3) rate constants converted from SSDRs; and (4) rate constants from existing models.

3.3.1. Comparison with literature-based estimates

An examination of plastic debris with identifiable production dates shows that over 70% of the secondary

microplastics collected from the ocean surface—primarily PE and PP—originate from the fragmentation of macroplastic objects manufactured in the 1990s or earlier (Lebreton et al., 2019). This suggests that t_{macro} for PE and PP in the water surface compartment likely exceeds 30 years, with the model estimate for PP (35 years) being in agreement with this. Moreover, the authors estimated that about 3% of the mass of positively buoyant macroplastics (e.g., PE and PP) fragment into microplastics each year, corresponding to a rate constant of 8.22×10^{-5} d^{-1}. The computed fragmentation rate constant for PP containers at the water surface is 1.94×10^{-5} d^{-1}, representing about 24% of the literature estimate. However, as the difference remains within one order of magnitude, the modeled value is deemed to be in reasonable agreement with the literature estimate. The overall lifespan of conventional fossil-based plastics has been estimated to range from about 100 to 1000 years (Kumari et al., 2025), within which the estimated t_{total} is expected to fall. Yet, t_{total} is below 100 years in certain compartments for PP and PS (Table 3), mostly the non-water compartments where UV and/or microbial activity is high. This may be because the literature estimates were mostly representative of water-comapartment litter, or it may indicate that the modeled degradation rate constants are overestimated. In the latter, the discrepancy may stem from the UV or thermal pretreatment of plastic samples applied in all biodegradation studies included in the database, which accelerates the process, and from the lack of blank controls in about 30% of the data points, which would otherwise correct for mass loss caused by the leaching of additives, unpolymerized residues, and other impurities.

3.3.2. Comparison with inseparable mass loss data

The model was applied to predict the total mass loss of PP and PS films (7.5 cm × 15 cm × 0.05 mm) due to fragmentation and degradation, and the results were compared with the combine and inseparable mass loss reported in the study by Hoseini et al. (2023). The lower bound of the 95% CI for mass loss was determined using the lower bounds of the 95% CIs for both the fragmentation and degradation rate constants, with the same procedure applied to determine the upper bound. Compared with the reported mass loss of 36.8% (for PP) and 1.1% (for PS) after 41 days of exposure, the model produces a lower estimate for PP (7.7%) and a higher one for PS (61.7%) (Table 4). This discrepancy may reflect an underestimated degradation rate constant of PP and an overestimated fragmentation rate constant of PS. These findings underscore the need for cautious interpretation of the model outputs, even for those deemed reliable (i.e., with high level of confidence), and even though the data quality of this single study is not assessed and could also be the source of the discrepancy

Table 4. Comparison of the overall mass loss of plastic films (7.5 cm × 15 cm × 0.05 mm) after 41 days of UV exposure, as estimated by PlasticFADE and reported by Hoseini et al. (2023)

Polymer	k_{frag} **[d^{-1}]**	k_{degr} **[d^{-1}]**	**Mass loss (model) [%]**	**Mass loss (model, 95% CI) [%]**	**Mass loss (reported) [%]**
PP	1.88E-03	6.37E-05	7.7	0.2 ~ 100.0	36.8
PS	2.35E-02	8.54E-06	61.8	60.7 ~ 63.0	1.1

3.3.3. Comparison with SSDR-based rate constants

Based on SSDR data provided by Chamas et al. (2020) and Maga et al. (2022), Corella-Puertas et al. (2023) derived degradation rate constants for microplastics in the ocean under different scenarios—fast, medium, and slow, by fitting first-order degradation kinetics to the reported SSDRs, converting them into bulk

degradation rate constants. Using the same input conditions, we applied PlasticFADE to compute degradation rate constants of five polymers and compared the outputs with the SSDR-based estimates (Fig. 4). The rate constants from PlasticFADE are presented as red dots with 95% CIs. Whereas Corella-Puertas et al. (2023) treated marine water as a single compartment, PlasticFADE distinguishes between the water surface and the water column to account for the difference in environmental stressors acting on plastics. The variation in the modeled rate constants between the two compartments highlights the importance of addressing them separately. Notably, the modeled rate constants for the water column align more closely with the SSDR-based values (Fig. 4b). The underlying data for SSDRs primarily originate from biodegradation rather than photooxidation studies. Since biodegradation prevails in the UV-absent water column, the observed alignment further validates the reliability of model results. For HDPE and LDPE, the rate constants exhibit no sensitivity to the SA:V, as illustrated in Fig. 4 and reflected by an estimated τ_i of less than 1×10^{-10} (Table S5, Supporting Information 1). This indicates that the effect of τ_i may have been compensated by other parameters during curve fitting, likely due to the limited variability in SA:V among the degradation data points for these two polymers. It is also important to note that degradation in PlasticFADE is not restricted to surface processes, whereas the SSDR approach assumes degradation occurs only at the surface of plastics, thus, the influence of the SA:V ratio on degradation is more important in the SSDR approach than in this study (Maga et al., 2022). Chamas et al. (2020) showed that assuming a constant or changing over time SA:V leads to computed lifetimes in the same order of magnitude, yet, the calculated lifetime was found to be smaller with a constant SA:V than with a changing one.

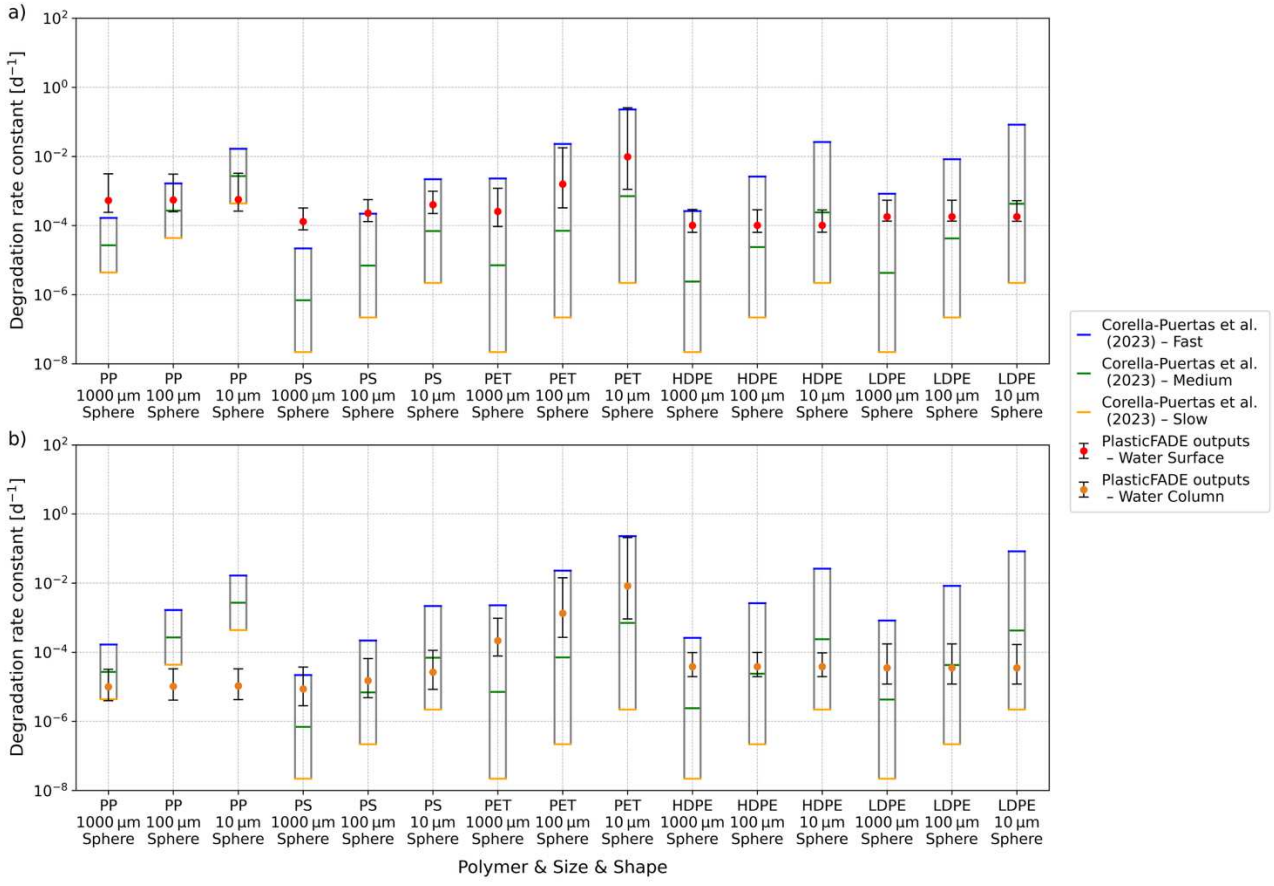


Figure 4. Comparison of modeled degradation rate constants for a) water surface and b) water column with

literature estimates for the marine water compartment

3.3.4. Comparison with rate constants from existing models

This section compares PlasticFADE with existing models, including environmental fate models of plastics (Domercq et al., 2022; Quik et al., 2023) and specialized models of fragmentation or degradation (An et al., 2021; Chamas et al., 2020; Kaandorp et al., 2021). Table 5 summarizes the polymers, particle sizes, shapes, and compartments considered in each model, as well as whether the dependence of rate constants on each factor is addressed. As shown in Table 5, PlasticFADE is the only model that accounts for the influence of all factors on fragmentation and degradation rate constants. A comparison of the rate constants among these models is provided in Fig. 5, excluding the SSDR-based estimates already shown in Fig. 4. When polymer type, shape, or size was not specified (Fig. 5), default inputs were applied in the calculation of rate constants using PlasticFADE: PP for polymer type, sphere for shape, and a diameter of 1000 μm for size. In contrast to existing models that provide only point estimates, PlasticFADE yields 95% CIs for all rate constants (Fig. 5), enabling quantitative assessment of model uncertainty and a more robust interpretation of model results.

Table 5. Comparison of PlasticFADE with existing models (FRAG: fragmentation, DEGR: degradation)

Model	**Coverage**	**Polymer**	**Size & shape**	**Compartment**	**Dependence**
PlasticFADE (This study)	FRAG & DEGR	PP, PS, EPS, PET, HDPE, LDPE, PE	Macro, micro, nano; Sphere, cube, film, fiber, irregular	Air, topsoil, subsoil, beach, water surface, water column, sediment	Polymer, size & shape, compartment
The Full Multi (Domercq et al., 2022)	FRAG & DEGR	Not specified	Micro and nano; Sphere	Surface water, flowing water, stagnant water, sediment top layer	Size & shape, compartment (FRAG only)
SimpleBox4Plastic (Quik et al., 2023)	FRAG & DEGR	Not specified	Micro and nano; Shape not specified	Air, water, soil, sediment	Compartment
Cascading FRAG (Kaandorp et al., 2021)	FRAG	Not specified	Not specified	Ocean, coast, beach	None
SSDR (Corella-Puertas et al., 2023)	FRAG	PP, PS, EPS, PET, etc. (13 in total)	Micro and nano; Sphere, film, fiber	Marine water	Polymer, size & shape
Multifactor Aging (An et al., 2021)	DEGR	PP, PE	Not specified	Air	Polymer

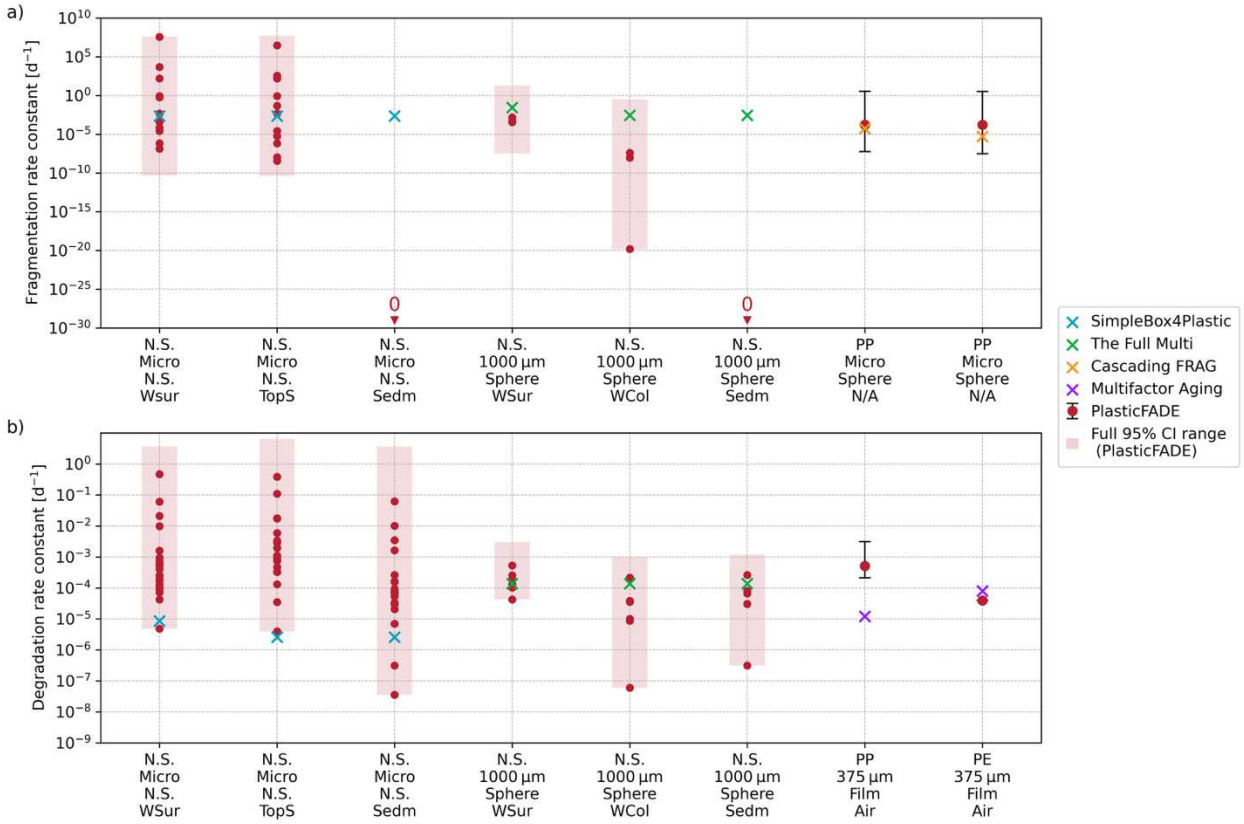


Figure 5. Comparison of a) fragmentation and b) degradation rate constants from PlasticFADE with existing models (SimpleBox4Plastic, The Full Multi, Cascading FRAG, and Multifactor Aging). X-axis labels (descending order) indicate polymer, particle size, shape, and compartment (N.S. = not specified; WSur = water surface; TopS = topsoil; Sedm = sediment; WCol = water column; N/A = not applicable). When the polymer (and size) is not specified in the existing model, PlasticFADE rate values for all polymers (and sizes) are shown as individual red dots, with the light red shaded envelope representing the full range between the minimum lower bound and maximum upper bound of all 95% confidence intervals. The compartment for Cascading FRAG is listed as N/A because the original study reports only stressor types and magnitudes without specifying the compartment.

3.5. Environmental interpretation

By further examining the modeled rate constants for the food container case, we derived relative rankings of fragmentation and degradation rate constants across polymers and compartments. Rate constants, expressed in d^{-1}, represent the relative mass loss per day due to fragmentation or degradation. Based on the geometric mean of the rate constants for each polymer, the estimated ranking (for the same compartment) from fastest to slowest is EPS > PP > PS for fragmentation, and PP > LDPE > PET > HDPE > PS > PE for degradation. These rankings should be interpreted with caution, as they depend strongly on the characteristics of the plastic samples applied in the experiments (e.g., whether they originate from pristine or post-consumer products). Similarly, by calculating the geometric mean of the ratios of rate constants between compartments for each polymer, we obtained the following ranking (fastest to slowest): for fragmentation—beach > air > water surface > topsoil > water column; for degradation—topsoil > beach > subsoil > water surface > air > sediment > water column (topsoil > beach > water surface > air for polymers

without identified degrading enzymes). Mechanical stress and UV intensity are highest on beaches, explaining the observed ranking for fragmentation. For degradation, although UV exposure is also greatest on beaches, microbial concentration is higher in topsoil, resulting in slightly faster degradation in this compartment. These rankings may change once regionalized environmental parameters are integrated into the model, as they are sensitive to inputs that can significantly vary across regions. The variation in rate constants spans several orders of magnitude across both polymers and compartments, with fragmentation showing a larger overall variability than degradation. For fragmentation, environmental conditions have a stronger influence on the modeled rate constants than polymer properties. For degradation, however, the relative influence of polymer versus compartment is less conclusive. Details of the corresponding data analysis are provided in the Excel sheet "Rate constants" in Supporting Information 2.

3.6. Implications for LCA

In LCA research, multiple studies have used simplified assumptions regarding fragmentation to estimate microplastics release, as fragmentation models are lacking (Askham et al., 2026; Corella-Puertas et al., 2023; Galafton et al., 2025; Louvet et al., 2026; Schwarz et al., 2024). To link emissions of macroplastics into the environment to emission of microplastics (and to apply the corresponding CFs), it is necessary to estimate how much of the debris fragment, as degradation and fragmentation occur as competing processes on macroplastics, where fragmentation is the only one that leads to microplastics generation. To that end, the mass balance equations were solved for microplastics generation as a function of time in Section S5 of Supplementary Information 1. The resulting equation was applied to PS and PP, the only polymers for which both degradation and fragmentation empirical constants are available A simplifying hypothesis is made using thickness/SA:V to create two categories for packaging materials: "flexible" (thickness: 0.8 mm, high SA:V ratio: 500 cm^{-1}) and "rigid" (thickness: 0.04 mm, low SA:V: 25 cm^{-1}) (Section S6 of Supplementary Information 1). The results suggest that flexible (i.e., thin) plastics tend to reach high fragmentation percentages: 80 to 100% of the initial macroplastic mass fragments (the rest being degraded directly from the macroplastic). For rigid (i.e., thicker) plastics, high fragmentation percentages of 30% (PP) and 80% (PS) are reached only on the beach, where UV intensity is the highest, and in other compartments, only 0 to 5% fragmentation is achieved. For both rigid and flexible plastics, values are highly uncertain in sediments and subsoil, where neither UV radiation nor mechanical stress is present. As a result, fragmentation is not expected to occur, and PS and PP, which lack known degrading enzymes in the environment, also exhibit negligible degradation. Thus, both fragmentation and degradation rates are null, making it impossible to estimate a fragmentation percentage other than 0 in these compartments. Yet, it is expected that plastics reach these compartments after redistributing from other compartments where fragmentation would have started (e.g. in water surface, before reaching water column and sediments). To obtain a better understanding of microplastics generation from macroplastics, a complete fate model for macroplastics (quantifying transfers between compartments) would be necessary to estimate the fate of macroplastics in the different environmental compartments where fragmentation and degradation occur at different rates. The fragmentation percentages for flexible and rigid macroplastics, PS and PP, in all environmental compartments are provided in Table S10 of Supplementary Information 1 and can be used as a first estimate in LCA studies of plastics which attempt to include microplastics emissions from fragmentation. The classification of flexible vs rigid packaging using only thickness is of course not representative of all packaging types, but considering the very sparse data regarding packaging material in LCA, this first categorization may support the integration of packaging impacts and drive data collection.

3.7. Limitations, recommendations, and outlook

This study makes a preliminary effort to develop a comprehensive model for estimating emission-specific fragmentation and degradation rate constants of plastics, and this section outlines the key limitations of the model. First, several assumptions and simplifications were introduced, particularly during model definition and the quantification of experimental and real-world environmental stresses. In fact, constant SA:V ratios, and fragmentation and degradation rates are assumed to calibrate the model, given the short timespan of the experiments used. Second, the dataset employed for model calibration were insufficient to ensure robust parameter estimation for each polymer considered, as fragmentation and degradation data is scarce in the literature. Third, fragmentation and degradation were modeled separately, without accounting for potential synergistic effects between these processes. Fourth, the effects of plastic additives on degradation and fragmentation were not accounted for due to a lack of data, but could influence these rates. This is further associated with the diverse origins of the plastic materials used across the experimental data sources.

To enhance data quality, we recommend systematically including appropriate blank controls and providing complete transparency regarding any pretreatments of the plastic samples in fragmentation and degradation studies. Tracking carbon fate (e.g., conversion to carbon dioxide or methane) in degradation experiments is also advised, as it offers a more reliable indicator of degradation-induced mass loss than comparing initial and final sample masses alone. Further, using 95% CIs alongside the point estimates is encouraged to gain insight into the lifespan of plastics in each environmental compartment. The PlasticFADE GitHub repository will be updated as additional data becomes available that can be used to calibrate empirical constants for extra polymers, or to refine existing constants. Future studies could explore machine learning approaches that integrate polymer properties (e.g., molecular weight, crystallinity, etc.) along with environmental parameters to predict degradation and fragmentation rates, potentially enabling generalizable models that do not rely on polymer-specific empirical constants.

Despite their limits and uncertainties, the rate constants computed by PlasticFADE represent a significant step toward filling existing data gaps in the current LCIA framework of plastic emissions. Compartment-specific degradation rate constants can replace the generic preliminary estimates currently used, thereby enabling more granular evaluations of plastic removal in relation to its fate. The integration of fragmentation rate constants further allows the assessment of impacts associated with secondary microplastics, which is not yet possible in the current framework. Moreover, the rate constants can be applied within multimedia fate models such as The Full Multi and SimpleBox4Plastic to enhance the representation of fate processes that occur within a single compartment. In terms of outlook, the model could be refined by expanding the range of polymers covered, incorporating temporal dynamics (e.g., changes in SA:V over time and their influence on rate constants), and addressing spatial heterogeneity through the regionalization of environmental stresses. In addition, integrating mechanistic insights into the model could enhance its predictive accuracy and explanatory power.

Declarations

Availability of data and materials

All data generated or analysed during this study are included in this published article and its supplementary information files. Any updates including additional degradation of fragmentation data that can be used to calibrate empirical constants for extra polymers, or to refine existing constants, will be uploaded to the GitHub repository: https://doi.org/10.5281/zenodo.19358104.

Competing interests

The authors declare that they have no competing interests.

Funding

This work received funding from Cotton Incorporated.

Authors' contributions

YT gathered and curated the data, calibrated the model, analyzed the results and wrote the original draft. NS and JL discussed implications for LCA and reviewed and edited the manuscript. AMB obtained funding and contributed to the conceptualization, methods and analysis of the model. All authors read and approved the final manuscript.

Acknowledgements

The authors gratefully acknowledge Cotton Incorporated for funding this project. We thank Prof. Michel Perrier for his valuable feedback and guidance on model definition and calibration. We also wish to express our appreciation to Dr. Christian Lott and Dr. Miriam Weber (HYDRA Marine Sciences) for sharing their expertise on plastic degradation. Finally, we extend our gratitude to Dr. Elena Corella-Puertas for her constructive input and insightful discussions throughout this study.

ChatGPT was used to polish the English language for improved readability. The content was subsequently reviewed and edited by the authors as needed.

Ethics declaration

Not applicable.

References

An, Z. H., Ye, Y., Xu, Z. P., & Yang, R. (2021). Study on Multi-factor Coupling Aging Kinetics of Polyolefins: Yearly and Monthly Aging Speed Maps. *Acta Polymerica Sinica*, *52*(11), 1514–1522.

Askham, C., Deville, A., Silva, M., Vázquez-Rowe, I., Boulay, A.-M., Corella-Puertas, E., Saadi, N., Pauna, V., Verones, F., & Kahhat, R. (2026). Expanding life cycle impact assessment to account for marine plastic emissions: A case study for the fishing industry. The International Journal of Life Cycle Assessment, 31(1), 46.

Auta, H. S., Abioye, O. P., Aransiola, S. A., Bala, J. D., Chukwuemeka, V. I., Hassan, A., Aziz, A., & Fauziah, S. H. (2022). Enhanced microbial degradation of PET and PS microplastics under natural conditions in mangrove environment. *Journal of Environmental Management*, *304*, 114273.

Bergmann, M., Mützel, S., Primpke, S., Tekman, M. B., Trachsel, J., & Gerdts, G. (2019). White and wonderful? Microplastics prevail in snow from the Alps to the Arctic. *Science Advances*, *5*(8), eaax1157.

Boucher, J., & Friot, D. (2017). *Primary Microplastics in the Oceans: A Global Evaluation of Sources*. Gland, Switzerland: IUCN.

Chamas, A., Moon, H., Zheng, J., Qiu, Y., Tabassum, T., Jang, J. H., Abu-Omar, M., Scott, S. L., & Suh, S. (2020). Degradation Rates of Plastics in the Environment. *ACS Sustainable Chemistry & Engineering*, *8*(9), 3494–3511.

Chow, J., Perez-Garcia, P., Dierkes, R., & Streit, W. R. (2023). Microbial enzymes will offer limited solutions to the global plastic pollution crisis. *Microbial Biotechnology*, *16*(2), 195–217.

Colwell, J., Pratt, S., Lant, P., & Laycock, B. (2023). Hazardous state lifetimes of biodegradable plastics in natural environments. *Science of The Total Environment*, *894*, 165025.

Corella-Puertas, E., Hajjar, C., Lavoie, J., & Boulay, A.-M. (2023). MarILCA characterization factors for microplastic impacts in life cycle assessment: Physical effects on biota from emissions to aquatic environments. *Journal of Cleaner Production*, *418*, 138197.

Domercq, P., Praetorius, A., & MacLeod, M. (2022). The Full Multi: An open-source framework for modelling the transport and fate of nano- and microplastics in aquatic systems. *Environmental Modelling & Software*, *148*, 105291.

Galafton, C., Budhiraja, V., Stevens, S., Mušič, B., & Maga, D. (2025). Environmental and littering impacts of disposable cups made of polypropylene and polylactic acid in Germany. Sustainable Production and Consumption, 57, 35–45.

Ghatge, S., Yang, Y., Ahn, J.-H., & Hur, H.-G. (2020). Biodegradation of polyethylene: A brief review. *Applied Biological Chemistry*, *63*(1), 27.

Hajjar, C., Bulle, C., & Boulay, A.-M. (2024). Life cycle impact assessment framework for assessing physical effects on biota of marine microplastics emissions. *The International Journal of Life Cycle Assessment*, *29*(1), 25–45.

Harrison, S., Uluseker, C., Pfohl, P., Santizo, K., Sipe, J., Lopez, B., Praetorius, A., Cross, R. K., Adediran, G. A., Svendsen, C., Wohlleben, W., & Wiesner, M. (2025). FRAGMENT-MNP: A model of micro-

and nanoplastic fragmentation in the environment. *Journal of Open Source Software*, *10*(110), 8061.

Hastie, T., Tibshirani, R., & Friedman, J. (2009). The elements of statistical learning.

Hoseini, M., Stead, J., & Bond, T. (2023). Ranking the accelerated weathering of plastic polymers. *Environmental Science: Processes & Impacts*, *25*(12), 2081–2091.

Kaandorp, M. L. A., Dijkstra, H. A., & Sebille, E. van. (2021). Modelling size distributions of marine plastics under the influence of continuous cascading fragmentation. *Environmental Research Letters*, *16*(5), 054075.

Law, K. L., Starr, N., Siegler, T. R., Jambeck, J. R., Mallos, N. J., & Leonard, G. H. (2020). The United States' contribution of plastic waste to land and ocean. *Science Advances*, *6*(44), eabd0288.

Lebreton, L., Egger, M., & Slat, B. (2019). A global mass budget for positively buoyant macroplastic debris in the ocean. *Scientific Reports*, *9*(1), 12922.

Louvet, J., Quik, J. T. K., & Boulay, A.-M. (2026). Regionalized characterization factors for microplastic emissions in life cycle assessment considering multimedia fate modelling. Journal of Cleaner Production, 538, 147217.

Ly, A., Marsman, M., Verhagen, J., Grasman, R. P. P. P., & Wagenmakers, E.-J. (2017). A Tutorial on Fisher information. *Journal of Mathematical Psychology*, *80*, 40–55.

Maga, D., Galafton, C., Blömer, J., Thonemann, N., Özdamar, A., & Bertling, J. (2022). Methodology to address potential impacts of plastic emissions in life cycle assessment. *The International Journal of Life Cycle Assessment*, *27*(3), 469–491.

Meng, X., Qiu, J., Zhang, B., Sakai, E., Zhang, L., Feng, H., & Tang, J. (2025). Thermal properties, mechanical performance, and environmental degradation behavior of polylactic acid and polyvinyl alcohol blends. *Polymer Bulletin*.

Merga, L. B., Redondo-Hasselerharm, P. E., Van Den Brink, P. J., & Koelmans, A. A. (2020). Distribution of microplastic and small macroplastic particles across four fish species and sediment in an African lake. *Science of The Total Environment*, *741*, 140527.

Mistry, A. N., Kachenchart, B., Wongthanaroj, A., Somwangthanaroj, A., & Luepromchai, E. (2022). Rapid biodegradation of high molecular weight semi-crystalline polylactic acid at ambient temperature via enzymatic and alkaline hydrolysis by a defined bacterial consortium. *Polymer Degradation and Stability*, *202*, 110051.

Pfohl, P., Wagner, M., Meyer, L., Domercq, P., Praetorius, A., Hüffer, T., Hofmann, T., & Wohlleben, W. (2022). Environmental Degradation of Microplastics: How to Measure Fragmentation Rates to Secondary Micro- and Nanoplastic Fragments and Dissociation into Dissolved Organics. *Environmental Science & Technology*, *56*(16), 11323–11334.

Quik, J. T. K., Meesters, J. A. J., & Koelmans, A. A. (2023). A multimedia model to estimate the environmental fate of microplastic particles. *Science of The Total Environment*, *882*, 163437.

Reineccius, J., Schönke, M., & Waniek, J. J. (2023). Abiotic Long-Term Simulation of Microplastic Weathering Pathways under Different Aqueous Conditions. *Environmental Science & Technology*, *57*(2), 963–975.

Saadi, N., Lavoie, J., Fantke, P., Redondo-Hasselerharm, P., & Boulay, A.-M. (2025). Including impacts of microplastics in marine water and sediments in life cycle assessment. *Journal of Cleaner Production*, *520*, 146037.

Schwarz, A. E., Herlaar, S., Cohen, Q. M., Quik, J. T. K., Golkaram, M., Urbanus, J. H., van Emmerik, T. H. M., & Huijbregts, M. A. J. (2024). Microplastic aquatic impacts included in Life Cycle Assessment. Resources, Conservation and Recycling, 209, 107787.

Sharp, J. A., Browning, A. P., Burrage, K., & Simpson, M. J. (2022). Parameter estimation and uncertainty quantification using information geometry. *Journal of The Royal Society Interface*, *19*(189), 20210940.

Sipe, J. M., Bossa, N., Berger, W., Von Windheim, N., Gall, K., & Wiesner, M. R. (2022). From bottle to microplastics: Can we estimate how our plastic products are breaking down? *Science of The Total Environment*, *814*, 152460.

Song, Y. K., Hong, S. H., Eo, S., Han, G. M., & Shim, W. J. (2020). Rapid Production of Micro- and Nanoplastics by Fragmentation of Expanded Polystyrene Exposed to Sunlight. *Environmental Science & Technology*, *54*(18), 11191–11200.

Song, Y. K., Hong, S. H., Eo, S., & Shim, W. J. (2022). The fragmentation of nano- and microplastic particles from thermoplastics accelerated by simulated-sunlight-mediated photooxidation. *Environmental Pollution*, *311*, 119847.

Tournier, V., Duquesne, S., Guillamot, F., Cramail, H., Taton, D., Marty, A., & André, I. (2023). Enzymes' Power for Plastics Degradation. *Chemical Reviews*, *123*(9), 5612–5701.

Woods, J. S., Verones, F., Jolliet, O., Vázquez-Rowe, I., & Boulay, A.-M. (2021). A framework for the assessment of marine litter impacts in life cycle impact assessment. *Ecological Indicators*, *129*, 107918.

Yang, W., Liu, R., Li, C., Song, Y., & Hu, C. (2021). Hydrolysis of waste polyethylene terephthalate catalyzed by easily recyclable terephthalic acid. *Waste Management*, *135*, 267–274.

Yottakot, S., & Leelavatcharamas, V. (2019). Isolation and Optimisation of Polylactic Acid (PLA)-packaging-degrading Actinomycete for PLA-packaging Degradation. *Pertanika Journal of Tropical Agricultural Science*, *42*(3), 1119–1129.

Zhang, K., Hamidian, A. H., Tubić, A., Zhang, Y., Fang, J. K. H., Wu, C., & Lam, P. K. S. (2021). Understanding plastic degradation and microplastic formation in the environment: A review. *Environmental Pollution*, *274*, 116554.

Supplementary Files

This is a list of supplementary files associated with this preprint. Click to download.

- SupportingInformation1PlasticFADE.docx
- SupportingInformation2PlasticFADE.xlsx